PAPER

Check for updates

Reducing attachment of marine diatoms and bacteria by fine tuning the modulus of PDMS based coatings

Thorsten Marochow, [ID] [a] Lejla Jusufagic,[a] John A. Finlay,[b] Peter Allen,[b] Anthony S. Clare [ID] [b] and Axel Rosenhahn [ID] *[a]

In recent years there has been an increase in the use of non-toxic fouling-release coatings to combat marine biofouling on the hulls of ships and a number of commercial products are established on the market. While fracture mechanics is considered to play a key role in the removal of macrofouling organisms, the effect of coating modulus on microfoulers is still poorly understood. A method to produce PDMS coatings with different moduli using a tin free condensation curing system has been established in our laboratory. The coatings were used to study the attachment of marine biofilm-forming organisms. Curing chemistry was investigated by solution and solid state ^{29}Si-NMR spectroscopy and the mechanical properties characterized by pendulum hardness tests. The coatings were tested against the attachment of three marine organisms *Ulva linza*, *Navicula perminuta* and *Cobetia marina*. The choice between dynamic and static assay conditions was found to be very important for soft fouling organisms. Under dynamic conditions, harder modulus coatings reduced the attachment of marine bacteria and diatoms.

Introduction

Surfaces immersed in natural aquatic systems tend to become fouled, first by a chemical conditioning layer and then by organisms that inhabit the local environment. This accumulation of biomass has a negative impact on a wide range of structures, for example ships' hulls,[1] aquaculture nets,[2] membranes for water treatment[3,4] and even biomedical devices in humans.[5] In the marine environment, this process of accumulation is very complex due to the huge diversity of species and their different interactions.[6,7] The formation of biofouling causes an increase in frictional drag and, in the case of ships higher fuel consumption.[8–10] Even light fouling, including that caused by smaller organisms like diatoms and bacteria, has a deleterious effect on cruising speed and causes a reduction in power of between 9% and 18%.[9,11] It was estimated that in 2018 1056 million tons of carbon dioxide emissions by the maritime sector were due to biofouling.[12] Avoiding biofouling is, therefore, not only important in economic terms, but also because of its effects on the environment and climate change.

One of the most common methods to prevent biofouling is the use of antifouling (AF) paints using toxic substances like copper oxides[13] or synthetic biocides.[14] All these paints tend to inhibit the accumulation of organisms, but also affect non-target species.[14–16] Fouling-release coatings (FRC) have shown great potential and mitigate the use of toxic ingredients. The aim of FRCs is to reduce the adhesion strength of organisms to the coating so that their removal from the surface can be readily accomplished even by weak shear forces generated by a cruising ship.[15]

Many different parameters affect the attachment and adhesion of organisms to surfaces and a large body of research has aimed to understand the way coating characteristics can be manipulated to produce more effective coatings.[16,17] The release of attached macrofoulants (*e.g.* barnacles or mussels) and the mechanisms involved in the failure of the joint between the organism and the coating have been studied intensively.[18–21] The main characteristics found to effect the attachment strength of organisms on a FRC are the elastic modulus E and the free surface energy γ.[22] The critical surface tension of polydimethylsiloxane (PDMS) films required to reduce the attachment strength of organisms is in the range of 20 to 30 mN m^{-1}.[23] Moreover, the low elastic modulus of many PDMS-based coatings is beneficial for low adhesion strength of macrofoulants. The square root of the product of surface energy and elastic modulus shows a strong relationship with organism adhesion strength.[24]

[a] *Analytical Chemistry – Biointerfaces, Ruhr University Bochum, 44780 Bochum, Germany. E-mail: Axel.Rosenhahn@Ruhr-Uni-Bochum.de*

[b] *School of Natural and Environmental Sciences, Newcastle University, Newcastle upon Tyne NE1 7RU, UK*

This correlation was investigated using various PDMS-based coatings with a large range of moduli. The elastic modulus is determined by the crosslinking density, which can be controlled through alteration of the PDMS chain lengths or by the concentration of crosslinking agent added. A higher crosslinking density in general leads to a stiffer film.[25] The commercially available product Sylgard 184 has been widely used for these kinds of studies.[26–28] This hydrosilylation curing product is supplied as a two-part liquid component kit. One part containing the PDMS and the other one containing crosslinker and catalyst in a fixed ratio. Changes in mixing ratios between both parts lead to variations in Young's modulus of between 9.0 and 0.02 MPa.[29,30] In another approach, hydrosilylation was used to cure a variety of PDMS oligomers with different chain lengths. The elastic moduli of these films were in a range of 9.4 to 0.2 MPa.[31] An alternative to the hydrosilylation process is condensation curing using tin- or titanium-based catalysts.[25] However, tin-based catalysts are toxic to many marine organisms at a concentration of 1 wt% and can interfere with the results of adhesion studies on living organisms.[32] Such coatings with moduli of 26 to 0.5 MPa have been used to investigate the adhesion of epoxy studs (pseudo-barnacles) as proxies for real barnacles.[33] Recently another approach used a tin-based condensation-cured process to cure tailored PDMS polymers with various chain lengths. In a two-step synthesis PDMS coatings were obtained with crosslinkable methoxy silane end groups. The range of Young's moduli for these coatings was within 0.3 and 3.2 MPa.[34]

Despite all of this work, the relationship between the modulus of a PDMS surface and the attachment strength of microfoulants has not been resolved. Chaudhury *et al.* (2005) established that the attachment strength of alga spores of *Ulva linza* did not correlate with modulus in the same way as it did for macrofoulers. There were no significant differences in spore removal for a 3-fold increase in modulus. Only an increase from 0.2 to 9.4 MPa (47-fold) showed significant differences in the number of spores removed. It was assumed that this was due to the adhesive pad of the spores deforming when a shear force was applied.[31] A recent field study also revealed that PDMS coatings with Young's moduli of 0.6 and 1.6 MPa outperformed softer coatings of less than 0.3 MPa when immersed in the Atlantic Ocean. This demonstrates that the buildup of marine biofilms on coatings cannot be correlated to the attachment strength of hard foulants alone and is far more complex.[34] However, the initial attachment of various pathogenic bacteria followed an inverted trend.[35] For example, an increase in modulus reduced the number of *E. coli* attaching under dynamic conditions significantly.[29] This correlation may also be relevant for improving the design of PDMS-based FRCs.

The formation of pathogenic biofilms under dynamic conditions can be correlated with the modulus of PDMS coatings.[29,35,36] In the present study, we explored the correlation between attachment of marine bacteria and diatoms under dynamic conditions and the settlement and release of algal zoospores on soft (≈ 1 MPa Young's modulus), condensation-cured PDMS coatings with moduli varying within a very narrow range. We present a customizable method to precisely tailor the Young's modulus by changing both the type of tin-free catalyst and the chain length of the bifunctional PDMS silanols. Using this method, six coatings were prepared whose outermost moduli varied only within a narrow and controlled range, which should have no significant effect on their FR properties against macrofoulants. To avoid the known toxic effects of tin, we chose two different titanium-based catalysts, titanium isopropoxide and titanium butoxide. To account for their moisture sensitivity, a precondensation step was established and verified *via* ^{29}Si-NMR. The mechanical properties of the coatings were characterized by means of pendulum hardness. Other physical and chemical properties of the films were determined *via* water contact angle (WCA) goniometry, ^{29}Si-MAS-NMR of the solid films, atomic force microscopy (AFM) and scanning electron microscopy (SEM). Finally, the correlation of pendulum hardness with the attachment of the marine diatom *Navicula perminuta* and the marine bacterium *Cobetia marina* under dynamic conditions was compared to the settlement and removal of the highly motile spores of *Ulva linza* under static conditions.

Materials and methods

Materials

Hexane ($\geq 95\%$) was purchased from VWR Chemicals and dried over molecular sieve. All other chemicals were used as purchased. Trimethoxymethylsilane (MTMS, 98%), titanium(IV) isopropoxide (TTIP, 97%) and titanium(IV) butoxide (TBOT, 97%) were purchased from Merck. The four silanols used DMS-S21 (90–120 cSt, 57 repeating units), DMS-S27 (700–800 cSt, 240 repeating units), DMS-S31 (1000 cSt, 350 repeating units) and DMS-S35 (5000 cSt, 660 repeating units) were purchased from Gelest and the average number of repeating units was determined *via* ^{29}Si-NMR.

PDMS film preparation

A series of PDMS films with different hardnesses was produced by condensation curing of PDMS using a fixed mass ratio between trimethoxymethylsilane (MTMS) and silanol terminated PDMS. The mass fractions of dry hexane, catalyst and one of the two silanols, which had a chain length of approximately 57 repeating units (as confirmed by ^{29}Si-NMR), were kept constant through all coatings. The concentration of the second silanol-terminated PDMS was varied to achieve the different crosslink densities and thereby pendulum hardnesses. The longer PDMS building blocks were estimated to have an average chain length of 240, 350 or 660 repeating units (^{29}Si-NMR). The catalysts chosen were titanium(IV) isopropoxide (TTIP) and titanium(IV) butoxide (TBOT). For film preparation, both silanols were mixed together and MTMS was added with vigorous stirring. Subsequently, the catalyst was premixed with dry hexane and added to the mixture. Precondensation of the compounds was achieved by stirring the mixture in a sealed flask for 24 h. Glass slides were mechanically cleaned and rinsed with ethanol and acetone. A 300 μm blade caster was

used to apply the liquid film to the cleaned glass slides. The films were dried at room temperature and controlled humidity (40–70%) for at least 72 h. Stability of the dried films was confirmed by repeating the pendulum hardness test after 12 weeks, showing only insignificant changes for almost all samples (results shown in SI).

Static contact angle goniometry

Determining water contact angles was done using a custom-built goniometer and previously published protocols.[37] Three measurements were performed on each of three replicates of each coating type. For each measurement, a droplet of tridistilled water was placed onto the film. Photographs of the droplets were acquired by using a charged-coupled device (CCD) camera. Contact angles were derived from the images using the Young's equation.

Pendulum hardness test

Hardness of the coatings was determined using a byko-swing pendulum hardness tester. To be compliant with ISO 1522, a König pendulum was used. The pendulum was deflected to $6°$ and released. The time for the swinging amplitude of the pendulum to decrease to $3°$ was recorded. Before measuring the films, the device was calibrated on pure glass with a pendulum hardness of 250 ± 10 s. Three measurements were made on three different replicate coatings of each type of PDMS. To assist in interpreting the measurements, pendulum hardness data for polyurethane elastomer (PUR) reference sheets with known tensile modulus are included in the plots shown in Fig. 2.

^{29}Si-NMR spectroscopy

All films were investigated in the liquid state after the 24 h precondensation step, just before application to glass slides, using a Bruker Ascend 400. To 350 μL of the uncured mixtures 350 μL CDCl$_3$, containing 18 mg mL^{-1} chromium(III) acetylacetonate, were added.[38] All purchased silanols were investigated by the same procedure. The crosslinking density of the cured films was determined by magic angle spinning (MAS) NMR spectroscopy using a Bruker DSX 400. The cured film was removed from a glass slide using a scalpel and added to a Bruker 4 mm VTN double resonance probe. Measurements were carried out with a MAS frequency of 10 kHz at room temperature.

Film thickness

The thickness of the films was determined by light microscopy using mechanically introduced scratches in the coating. The vertical height was calculated using the z-values of the microscope stage at the focus points on the blank substrate and on the top of the remaining film. For each type of film three replicates were analyzed at three different spots and the averages reported.

Atomic force microscopy

The roughness of the films was characterized by acquiring images via atomic force microscopy (AFM). A NanoWizard 3 (JPK, Germany) was equipped with an Multi75GD-G cantilever

and a setpoint of 2 V and a frequency of 1 Hz was chosen for the tapping mode. Images of a size of 40×40 μm (512×512 px) were measured at a scan speed of $31\,250$ nm s^{-1} at three different spots on each sample type. The roughnesses of the images were quantified as RMS values by using Gwyddion (Version 2.69).

SAM preparation

Self-assembled monolayers (SAMs) of 1-dodecanthiol (DDT) were used as reference surfaces for the bioaccumulation assays. These surfaces were prepared following previously published protocols.[39] The gold-coated glass slides (Georg Albert, PVD, Silz, Germany) were cleaned by treating with ozone for 1 h which was generated with an UV lamp. This was followed by ultra sonification in ethanol p.a. for 30 min before drying in a nitrogen stream. The monolayer was prepared by immersing the cleaned slides in a 1 mM ethanolic DDT solution for 24 h. After removal, the surfaces were rinsed with ethanol p.a., subjected to 3 min ultrasonication in ethanol p.a., before a final rinsing with ethanol p.a. After drying in a nitrogen stream, the SAM-coated slides were stored under argon until needed.

Bacterial culture

Accumulation assays with bacteria were done under dynamic conditions using *Cobetia marina*. The bacterial culture was received from Deutsche Sammlung von Mikroorganismen und Zellkulturen (DSMZ, Braunschweig, Germany). Overnight cultures were prepared in 7.5 mL sterile MB medium at 18 °C following previously published protocols.[39] After filtering, the suspension was diluted using MB medium to an OD$_{600}$ of 0.1. This was centrifuged for 3 min at 3000 rpm (Hettich Zentrifugen, Lauenau, Germany) and the pellet resuspended in nutrient-free artificial sea water (ASW) (pH 8.0) to give a final OD$_{600}$ of 0.01, corresponding to a concentration of 7.5×10^6 cells mL^{-1}.

Dynamic accumulation assay with bacteria

Previously published protocols were used to run the dynamic accumulation assays using the marine bacterium *Cobetia marina*.[40] The dried PDMS films and one replicate of a DDT SAM were each covered with 4 mL of sterile ASW and incubated for 1 h at 65 rpm on an orbital shaker (neolab DOS-10L). While shaking, 4 mL of bacteria solution were added and kept on the shaker for an additional 45 min. After this incubation step glutaraldehyde solution (2.5 vol% in water) was added to fix the bacteria and kept on the shaker for an additional 10 min. The samples were removed from the aqueous phase and washed twice by placing them in Milli-Q water on the shaker for 10 min each. For quantification of the bacterial densities, they were stained with a BacLight bacterial viability kit from Thermo Fisher Scientific (Molecular Probes, USA). Eighty fields of view were acquired for each sample by using fluorescence microscopy (Nikon Eclipse TE2000-U, 20× phase contrast objective Nikon CFI Plan Fluor DLL NA 0.3, Nikon, Tokyo, Japan) to quantify the attached bacteria. For each PDMS formulation, three replicates were analyzed. The statistical significance of observed differences was determined by a one-way ANOVA with *post hoc* Tukey analysis (significance level $\alpha = 0.05$).

Dynamic accumulation assay with diatoms

Accumulation assays with *Navicula perminuta* were performed following previously published protocols.[41] Samples were incubated in 4 mL sterile ASW for 1 h at 65 rpm on an orbital shaker (neolab DOS-10L). After filtering through a 70 μm sterile filter the suspension of diatoms was adjusted to a cell density of 4×10^6 cells mL^{-1} using sterile ASW. To each sample, 4 mL of the suspension was added and kept at 65 rpm for 1 h. Fixation of the diatoms was done by adding 0.9 mL of 25% glutaraldehyde in water and shaking for an additional 10 min. To remove non-attached diatoms and residues from the ASW, the samples were washed twice in Milli-Q water at 65 rpm for 10 min each. The slides were dried overnight in the dark at room temperature. Each sample was characterized by recording 80 fields of view, each of 0.55 cm^2 (Nikon Eclipse TE2000-U, 10× phase contrast objective Nikon CFI Plan Fluor DLL NA 0.3, Nikon, Tokyo, Japan). For each PDMS formulation, three replicates were analyzed. The spore density was normalized to the spore density on the SAM DDT slides used in the same assay. One-way ANOVA with *post hoc* Tukey analysis (significance level α = 0.05) was used to determine the statistical significance of observed differences.

Adhesion assay with *Ulva linza*

Plants of *Ulva linza* were collected from Craster, UK (55°26′ N; 1°35′ W) in north east England. Spores were released from the fronds using the method of Callow *et al.* (1997) and a spore suspension of 1.0×10^6 spores ml^{-1} was prepared.[42,43] Slides were covered with 10 ml of the suspension in individual compartments of quadriPERM dishes. After 45 min, the slides were gently washed to remove unsettled spores and the attached spores were fixed using 2.5% glutaraldehyde in ASW. The density of zoospores was determined using an image analysis system (Leica LASX) attached to a Zeiss Axioscope 2 Plus fluorescence microscope. For each coating type 90 counts on 3 replicates were evaluated.

Removal studies were carried out using a further 3 slides of each type settled with spores as described above. These were exposed to a shear stress of 52 Pa in a water channel for 5 min (Schultz *et al.* 2000). Samples were fixed and the number of cells remaining attached was counted as described above.

Results

To explore the fouling retention of soft coatings with different mechanical properties, a set of polydimethylsilloxane (PDMS) coatings was developed in which the choice of tin-free catalysts and the length of the base siloxane was varied. The reaction scheme is shown in Fig. 1(a). Silanol-terminated PDMS as the base of the coatings, was condensation crosslinked with MTMS using either titanium(IV) isopropoxide (TTIP) or titanium(IV) butoxide (TBOT) as catalyst. We deliberately chose a tin-free system to exclude any biocidal effects that might arise from different amounts of residual tin close to the surface of the coatings. Fig. 1(c) shows the three different silanol compositions used for each catalyst. To control the elasticity of the coatings, the chain length of the PDMS compounds was varied while the amount of the crosslinking MTMS was kept at 17 wt%. Damping times determined by pendulum hardness
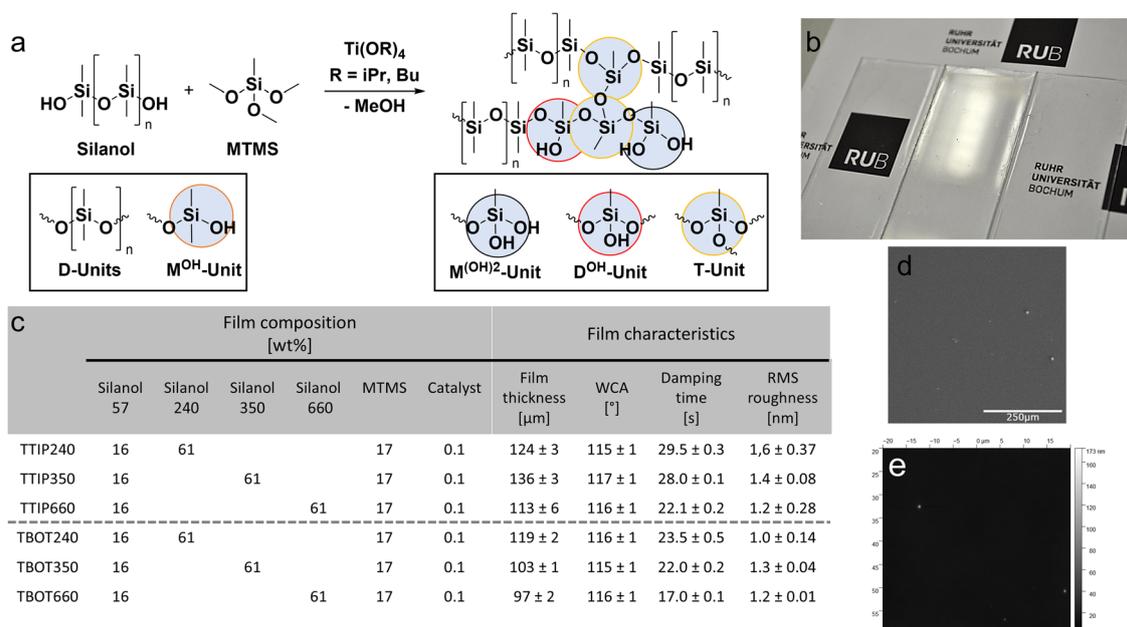

	Film composition [wt%]						Film characteristics			
	Silanol 57	Silanol 240	Silanol 350	Silanol 660	MTMS	Catalyst	Film thickness [μm]	WCA [°]	Damping time [s]	RMS roughness [nm]
TTIP240	16	61			17	0.1	124 ± 3	115 ± 1	29.5 ± 0.3	1,6 ± 0.37
TTIP350	16		61		17	0.1	136 ± 3	117 ± 1	28.0 ± 0.1	1.4 ± 0.08
TTIP660	16			61	17	0.1	113 ± 6	116 ± 1	22.1 ± 0.2	1.2 ± 0.28
TBOT240	16	61			17	0.1	119 ± 2	116 ± 1	23.5 ± 0.5	1.0 ± 0.14
TBOT350	16		61		17	0.1	103 ± 1	115 ± 1	22.0 ± 0.2	1.3 ± 0.04
TBOT660	16			61	17	0.1	97 ± 2	116 ± 1	17.0 ± 0.1	1.2 ± 0.01

Fig. 1 (a) Schematics showing the hydrolysis-condensation reaction of MTMS with PDMS silanols including four different silicone species from the initial compounds (D-units: silicone of the dimethylsiloxane repeating units, M-^{OH}-units resulting from the silicones terminating each PDMS) and those formed during the condensation process (M$^{(OH)2}$-units, D^{OH}-units and T-units resulting from MTMS after the first, second and third condensation step). (b) Image of the coated glass slides yielding fully transparent PDMS coatings. (c) Composition used to synthesize the films and their resulting physicochemical properties. (d) and (e) SEM and AFM images of TTIP660 showing a smooth surface with only minor defects.

test varied between 17 and 29 s (Fig. 1(c)). Determining the pendulum hardness after 12 weeks confirmed full curing for nearly all formulations (Fig. S9). The compositions, including the longest silanol with a chain length of about 660, resulted in the softest films. The film thickness of the dried, clear films was determined *via* light microscopy using a calibrated motorized unit focusing at a scratch that was applied to the thin PDMS films. All films had a dry thickness between 97 ± 2 and 136 ± 6 µm (Fig. 1(c)). Using the silanol with a chain length of 660 and TBOT resulted in the thinnest film with a thickness of 97 ± 2 µm, while the film with the shortest silanol 240 had a thickness of 119 ± 2 µm. Thus, within this series of samples the use of longer silanol resulted in thinner films. For the TTIP series no clear trend was found and the highest film thickness was obtained using the silanol with a medium chain length of 350 (136 ± 3 µm) and the lowest thickness was found for the silanol 660 (113 ± 3 µm). As a result of the curing process $M^{(OH)2}$-, D^{OH}-, or T-units can be formed, and their ratio depends on the degree of condensation of the MTMS. The composition of those units after the precondensation step and after complete curing of the coatings was investigated *via* ^{29}Si-NMR spectroscopy as described below. The wettability of all film compositions was determined by static water contact angle goniometry. Water contact angles (WCA) were in a very narrow range between $115 \pm 1°$ and $117 \pm 1°$ and showed great consistency between all formulations (Fig. 1(c)). The narrow range of wettability was important to restrict the analysis in this work to purely the mechanical properties and avoid any alterations caused by different surface chemistries. The cured films had a transparent and even appearance (Fig. 1(b)) and in high magnification SEM images an extremely smooth surface with very sparse defects (Fig. 1(d)). The impression from the SEM data was supported by AFM images revealing a smooth surface

for all samples, ranging from 1.6 ± 0.37 nm for TTIP240 down to only 1.0 ± 0.14 nm for TBOT240 (Fig. 1(e)). SEM and AFM images of all films are shown in (Fig. S7 and S10).

The mechanical properties of the PDMS films were characterized by pendulum hardness measurements. As shown in Fig. 2, the duration required to reduce the amplitude of a Koenig pendulum swinging on the PDMS coatings from 6° to 3° was measured as damping time or pendulum hardness in seconds. The damping time is known to be linearly correlated to the Young's modulus up to a certain point.[44] A series of commercial polyurethane (PUR) materials with known Young's modulus between 0.2 and 4.0 MPa (PUR0.2 to PUR4.0, Fig. 2(a)) was used to identify the region of linear correlation for the used setup. The inset in Fig. 2(a) shows the obtained values and reveals a linear correlation between the known Young's moduli of the reference PUR materials and the pendulum hardness ($R^2 = 0.99$). All PDMS films prepared in this work had a pendulum hardness in the range between the PUR references with 0.6 and 1.6 MPa modulus (Fig. 2(b)). While this comparison provides a good estimate of the moduli of the coatings, more precise correlations have to be done with a certain caution as the material characteristics might affect the pendulum hardness. The PDMS films cured using TTIP as catalyst ranged in pendulum hardness between 29.5 and 22.1 s. The hardest film resulting from TBOT had a reduced damping time of 23.5 s while the softest one had only a damping time of 17.0 s. Damping times of all films can be seen in Fig. 2(b). As expected, an increase in the chain length of the silanol used within a composition resulted in a decrease of the pendulum hardness of the resulting film. This correlates well with published values and is true for both types of catalyst used.[25]

^{29}Si-NMR was used to determine the conversion of M^{OH}-units and MTMS after 24 h precondensation right before casting the liquid composition to the cleaned glass slides.
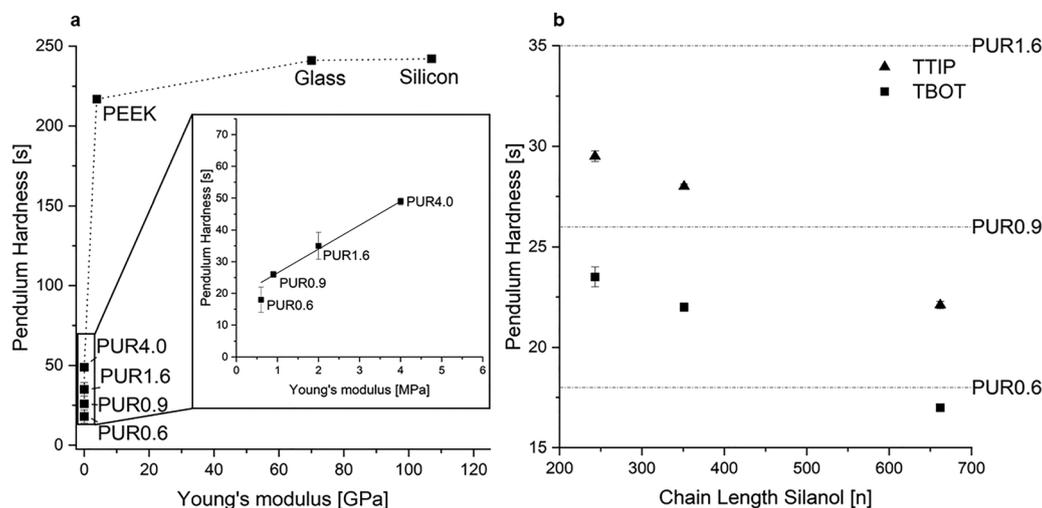

Fig. 2 Pendulum hardness measurements to characterize the mechanical properties of the PDMS coatings. (a) Pendulum hardness (Koenig) of reference materials (PEEK: Polyether ether ketone, Glass: unfunctionalized glass slides, Silicon: Silicon wafers, PUR: polyurethane elastomer, the number refers to its Young's modulus) in relation to their known Young's modulus. The inset shows a proportional relationship between Young's modulus and pendulum hardness below 50 s ($R^2 = 0.99$). (b) Pendulum hardness (Koenig) of the cured films for the different chain lengths of the longer silanol compound in the composition. The dotted lines show the pendulum hardness values of the PUR references with a Young's modulus of 0.6, 0.9 and 1.6 MPa.

Fig. 3 shows the deconvoluted ^{29}Si-spectra of TTIP240 and TBOT240 in different curing states. In the spectra of the composition before adding the catalyst the signal of M^{OH}-units of the silanols appeared at −11 ppm, D-units of the PDMS chains had a chemical shift of −22 ppm and the silicon atom of the MTMS had a chemical shift of −39 ppm. After 24 h precondensation, a large amount of the MTMS could still be seen at −39 ppm (TTIP240 24 h and TBOT240 24 h in Fig. 3). Next to this, four signals were present representing different reaction products of MTMS. $M^{(OR)2}$-units resulting from MTMS molecules which have been condensed once (−48 ppm) and do not increase the crosslinking density. D^{OR}-units resulting from MTMS molecules that are bound to two different silicon atoms (−57 ppm) and thereby might interconnect two PDMS silanols, increasing their chain length significantly and T-units resulting from MTMS molecules which are fully integrated into the silicone network (−67 ppm). The T-units increase the cross-linking density of the PDMS mixture. It should be noted that only TBOT showed the presence of a significant number of D^{OR}-units within its spectra, indicating an increase in PDMS chain length rather than the formation of a cross-linked network. An increase in chain length within a cured coating is known to decrease its elastic recovery.[25] Next to those three species, a fourth one occurred between −40 and −42 ppm (expansion Fig. 3). Within the TBOT compositions, the signal was found at −40 ppm while in compositions containing TTIP only a signal at −42 ppm was observed. These signals could indicate different condensation species containing the catalysts. Comparison between the four different condensation products of MTMS and the uncondensed MTMS revealed different conversion rates shown in Table 1. After a period of 24 h the conversion rates of MTMS in both of the mixtures containing the shortest silanol were at their highest at 10% and 11%, respectively. This may be related to viscosity effects slowing the reaction in the samples

Table 1 Conversion of MTMS and silanols after 24 h stirring in a sealed flask. All spectra are shown in the SI

Sample	MTMS conversion (%)	Silanol conversion (%)
TTIP240	11	75
TTIP350	5	67
TTIP660	6	71
TBOT240	10	76
TBOT350	7	68
TBOT660	7	65

with longer silanols, reducing the conversion of the MTMS to only 5 to 7%. However, in all samples at least 65% of the silanols of the PDMS compounds were converted after the precondensation. The cured films were investigated by ^{29}Si-MAS-NMR (TTIP240 cured and TBOT240 cured in Fig. 3). All films show a full chemical integration of MTMS into the silicone network, indicated by the absence of signals at −39 ppm. However, signals of M^{OH}- and D^{OR}-units are still notice-able, indicating some remaining and non-reacted groups. The increasing viscosity during the curing process might limit the diffusion and thus the completion of the reaction.

Antifouling properties

The influence of the mechanical properties of the silicone coatings on the attachment of three different marine organisms – algal zoospores, diatoms and bacteria – was investigated. *Ulva linza* zoospores were used to study attachment under static conditions and the release of attached spores when applying a shear stress of 52 Pa (Fig. 4), while attachment under dynamic conditions was examined using the marine diatom *Navicula perminuta* (Fig. 5) and marine bacteria *Cobetia marina* (Fig. 6).

For the *U. linza* experiments, zoospores were allowed to attach to the coatings for 45 min before the settlement densities were quantified (Fig. 4(a), gray bars). Within the TTIP series, TTIP240 had the lowest number of attached spores (222 mm^{-2}) followed by TTIP350 (273 mm^{-2}), and TTIP660 (279 mm^{-2}), albeit only TTIP240 was significantly different ($p < 0.05$). The films which were cured using TBOT (containing the longer silanols) showed less variation between spore densities than the TTIP series. Thus, neither the silanol chain length, nor the choice of catalyst showed an unequivocal effect on the settlement preference of *U. linza* zoospores. A second set of slides with settled spores was used to determine the relative adhesion strength of the spores. These were exposed to a wall shear stress of 52 Pa in a turbulent flow water channel and the spore density remaining attached was determined by micro-scopy (Fig. 4(a), blue bars). The cell counts revealed no sig-nificant difference ($p > 0.05$) between the samples (184 to 205 number per mm^2), except for TTIP350 on which the spore density remaining was slightly higher (239 mm^{-2}). Fig. 4(b) presents the relation between pendulum hardness and the number of spores which remained after applying the shear stress. TBOT660, TBOT350, TTIP350, and TTIP240 showed no significant differences in removal ($p > 0.05$). Only TTIP660 and TBOT240 showed a slightly enhanced removal of up to 30% (*versus* 13% of the other four coatings). Thus, again no
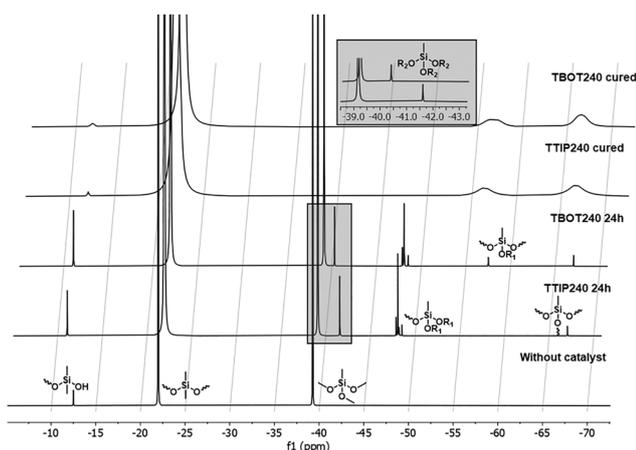

Fig. 3 Deconvoluted stacked ^{29}Si-NMR spectra of silanol MTMS mixture before adding the catalyst, liquid TTIP240 and TBOT240 after 24 h pre-condensation and ^{29}Si-MAS spectra of cured TTIP240 and TBOT240 films. R_1 = H or CH$_3$ and R_2 = H, CH$_3$ or titanium species. The spectra were normalized to the dominating dimethylsiloxane building blocks at −22 ppm and the spectral intensity are arbitrary units.
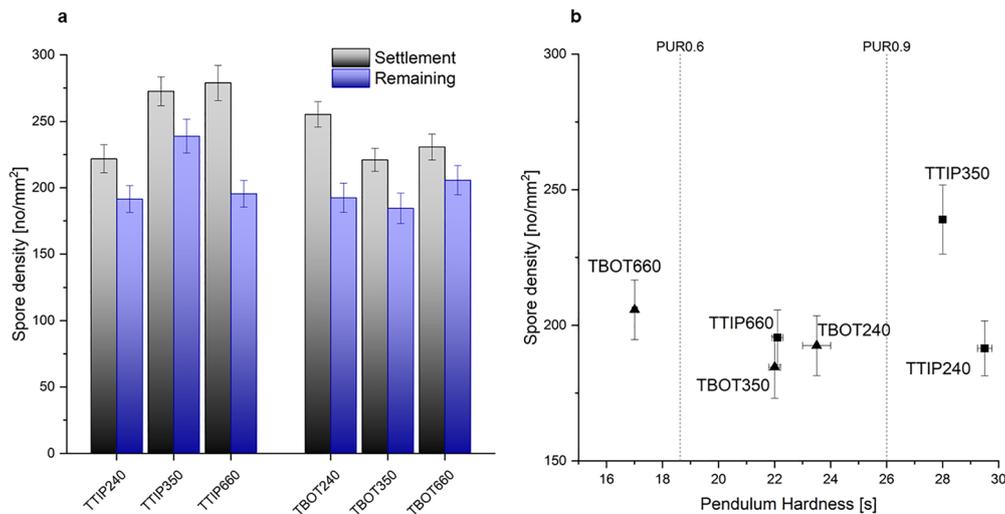
Fig. 4 (a) Density of attached zoospores of *Ulva linza* after 45 minutes settlement time and spores remaining after exposure to a shear stress of 52 Pa. (b) Remaining spores relative to the pendulum hardness of the PDMS films PCC = 0.16. Each point is the mean of 90 counts on 3 replicate slides. Bars show the 95% confidence limits.
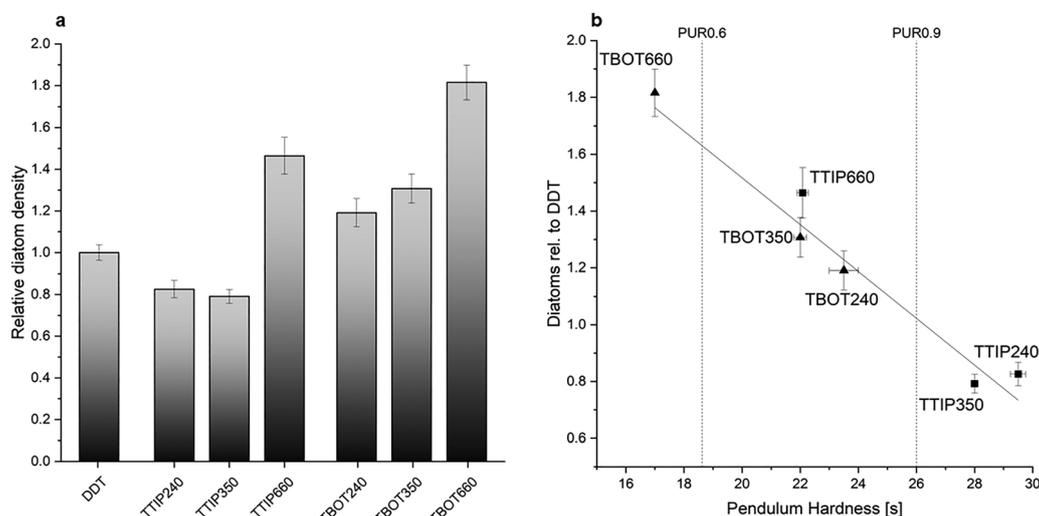

Fig. 5 (a) Result of the dynamic accumulation assay with diatoms *Navicula perminuta*. Average of three individual measurements are shown. Error bars show the standard error of the mean. (b) Correlation between attached diatoms *Navicula perminuta* and pendulum hardness (Koenig) PCC = −0.94.

systematic effect of pendulum hardness was found in relation to removal. The Pearson correlation coefficient (PCC) was 0.16.

Fig. 5(a) shows the density of *N. perminuta* cells on the films relative to a DDT reference after the dynamic accumulation assay. On TTIP660, 46% more diatoms attached than on the reference DDT sample. However, the films TTIP240 and TTIP350 reduced the attachment of diatoms by 17 and 21%, respectively. On all films cured with TBOT more organisms attached during the assay than on the reference sample DDT. While the difference between the reference sample and TBOT240 was not significant, the performance of TBOT350, and especially TBOT660, was significantly worse. The number of attached diatoms on TBOT660 was more than 81% higher than on the negative reference. Fig. 5(b) shows the correlation

between pendulum hardness and the attachment of *N. perminuta* within the dynamic accumulation assays. An increase in the film's pendulum hardness resulted in a reduced attachment of diatoms within the assay. Both TTIP- and TBOT-catalyzed films showed the same trend and there was no significant difference in the number of attached diatoms between TTIP660 and TBOT350, which had the same damping time of 22 s. With a Pearson correlation coefficient (PCC) of −0.94, there was a linear correlation between pendulum hardness and the number of attached diatoms, which was independent of the catalyst used.

Fig. 6(a) shows the attachment of the bacterium *C. marina* relative to DDT references under dynamic conditions. All films reduced the accumulation of bacteria relative to DDT. The
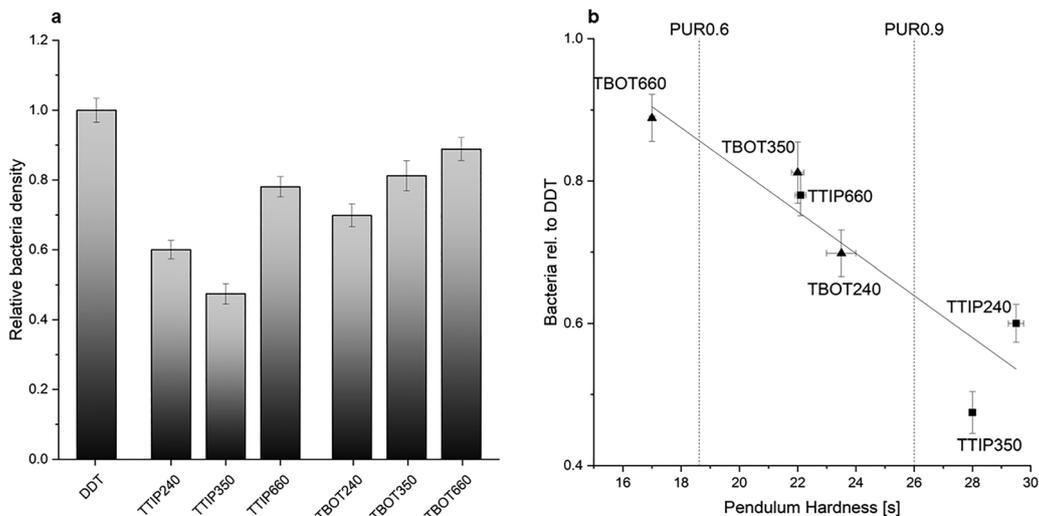
Fig. 6 (a) Result of the dynamic accumulation assay with bacteria *Cobetia marina*. The average of three individual measurements is shown. Error bars show the standard error of the mean. (b) Correlation between attached marine bacteria *Cobetia marina* and pendulum hardness (Koenig) PCC = −0.91.

TBOT series shows a linear correlation between the chain length of the silanol and accumulation of bacteria. While TBOT660 reduced the number of bacteria by 11%, TBOT350 and TBOT240 reduced them by 19% and 30%, respectively. No such trend could be observed for the films cured with TTIP. TTIP660 reduced the number of attached bacteria by 22% and TTIP240 reduced it by 40%, which agrees with the TBOT series but TTIP350 outperformed both other films by a reduction of 53%. The correlation between bacterial adhesion under dynamic conditions and pendulum hardness can be seen in Fig. 6(b). The adhesion of bacteria was decreased by higher pendulum hardness and thereby higher Young's modulus for most of the films. In contrast, TTIP240 has a higher pendulum hardness than TTIP350, but the reduction of accumulated bacteria decreased from 53 to 40%. However, the difference in bacterial densities was not statistically significant. Despite this, there was a linear correlation between all six samples (PCC = −0.91). The type of titanium catalyst used within the film had no impact on the dynamic attachment of *C. marina*. This was demonstrated by TBOT350 and TTIP660, which had the same pendulum hardness and showed no significant differences in bacterial attachment.

Discussion

In this work we present a robust method to produce soft PDMS-based thin film coatings with customizable mechanical properties, using a variety of PDMS silanols and catalysts. By varying the chain length of the difunctional silanols and the type of catalyst used in the condensation curing system, the coating composition could be tuned to produce coatings with a wide range of moduli. The pendulum hardness systematically decreased as the lengths of linear PDMS chains within the coatings increased, due to a reduction in elastic recovery. Common catalysts for condensation curing silicone coatings are tin-based alkoxides. As tin is known to be toxic to many marine organisms, it was replaced with a titanium alkoxide

catalyst system. Although this worked well, it was a challenge to overcome the catalyst's sensitivity to air moisture and its slower curing speed. Both drawbacks were met by including a pre-condensation step in a sealed vessel to reduce air humidity. ^{29}Si-NMR confirmed the success of this approach. In all formulations at least 65% of M^{OH}-Groups originating from the silanols were already condensed before application of the formulations to the substrate, which resulted in reduced curing times. All coatings were applied by blade casting with a wet thickness of 300 μm on cleaned glass slides. Complete curing on the substrate was achieved within 72 h at ambient temperature. ^{29}Si-MAS-NMR confirmed that after this curing period, 100% of the MTMS was covalently linked within the silicone matrix. The cured films looked clear and transparent with smooth, defect sparse surfaces as confirmed by SEM images. Dry film thicknesses were in a narrow range between 97 and 135 μm. No significant variations in wettability were observed since all water contact angles were between 115° and 117°, yet the pendulum damping time varied from almost 30 s down to only 17 s. These values are in the range of PUR reference materials with known elastic moduli. The investigated PDMS coatings had pendulum damping times which were within the regime which showed a linear correlation between elastic modulus (0.6 and 4.0 MPa) and pendulum hardness (18 and 49 s) (Fig. 2). Being aware that a direct comparison between different polymers must be carried out with caution, we can approximate the range of moduli of the PDMS coatings to be roughly between 0.5 and 1 MPa. In both, the TTIP and the TBOT catalyzed coating series, a linear correlation between silanol chain length and Young's modulus was found. One possible explanation for the softer TBOT films may be their tendency to more readily form D^{OH}-units within the precondensation reaction (Fig. 3). This increases the proportion of linear, non-branched components in the cured matrix and thereby reduces its elastic recovery.[25] Films crosslinked using TBOT resulted in a 21 to 23°% lower pendulum hardness and thus Young's

modulus than their TTIP catalyzed counterparts, while the relative hardness differences caused by a changed PDMS chain remained similar. The comparison between the compositions TTIP660 and TBOT350 are well suited to exclude any influence of the catalyst type on the attachment of the marine organisms as there were no significant differences between the damping times of these two coatings (22.1 s and 22.0 s, respectively).

The influence of the pendulum hardness on the AF and FR properties of the films under static conditions was investigated by settlement and removal assays of motile *Ulva linza* zoospores. There was no obvious correlation between PDMS chain length or the type of catalyst and the number of settled spores (Fig. 4). After applying a shear stress of 52 Pa by a turbulent water flow, 11 to 17% of the settled zoospores were removed from TTIP240, TTIP350, TBOT350, and TBOT660. Any differences between these four coatings in the assay were not statistically significant. Only TTIP660 and TBOT240 showed slightly increased spore removal compared to the other four formulations of 25 and 30%, respectively. Correlating the pendulum hardness of the coatings with the assay results reveals that there was no relationship between spore attachment or spore removal within the range of hardness used in this work. This is in good agreement with previous findings which showed that only large differences with a factor of 47 in elastic modulus have a compelling effect on the FR properties of PDMS-based coatings on soft foulants, while any correlation for hard foulants remained elusive.[31]

In contrast to the *U. linza* experiments, the dynamic attachment assays with the diatom *Navicula perminuta* (Fig. 5) and the marine bacteria *Cobetia marina* (Fig. 6) showed statistically significant differences in the number of attached organisms despite the moderate range of pendulum hardnesses tested. In both cases, a decreasing attachment density was observed with increasing pendulum hardness. The density of attached diatoms varied greatly between coatings, as on the softest TBOT660 coating more than doubled values were found compared to the hardest one, TTIP240. Assays with *C. marina* show that this effect seems also to be true for smaller organisms since an increase of attached bacteria of 50% on the softest compared to the hardest coating was observed. The general trend of decreasing attachment with increasing pendulum hardness found for both organisms is in good agreement with the known correlation for *E. coli* bacteria.[29]

At the moment we can only speculate why diatoms and bacteria attaching under dynamic conditions showed a much stronger difference in attachment on the different coatings than the self-propelled *U. linza* zoospores under static conditions. One major difference between the two assays is that zoospores actively swim with a velocity of about 150 μm s^{-1}[45] and search for a suitable settlement site. In addition, their velocity reduces by up to 70% when getting close to a surface.[46] The momentum of the spores is thus much smaller than that of the diatoms or bacteria, which were investigated under dynamic conditions at much higher velocities and thus a higher momentum. This difference in velocity could be the reason that the momentum for diatoms and bacteria is high enough to become sensitive to the reduced elastic recovery of the softer coatings. Because of this reduced elastic recovery, the dissipation of the kinetic energy of the small organisms colliding with the surface with a certain momentum may be higher. This would make it more likely that the organisms decelerate to an extent that they are able to attach to the surface. At first glance the results seem to be slightly contradictory to those published for the removal of barnacle and pseudo-barnacles for which the square root of the product of surface energy and elastic modulus showed a strong relationship with organism adhesion strength and thereby softer surfaces were advantageous in terms of fracture mechanics and removal from coatings.[21,24,31,47,48] We can only speculate that in our study the smaller size and the viscous properties of the biofilm formers were the reason that energy dissipation during the attachment of the organisms was the dominant effect.

Conclusion

Within this work we present a method by which the mechanical properties of PDMS-based coatings can be fine-tuned and characterized, by measuring their pendulum hardnesses. The production of coatings using the non-toxic titanium-based catalysts allows the study of attachment mechanisms of marine fouling organisms while avoiding the risk of biocidal effects of tin-based curing systems.[32] Results showed that the attachment density of marine diatoms and bacteria tested under dynamic conditions decreased with an increase in elastic modulus. Doubling the modulus of the coatings resulted in less than half the number of diatoms attaching to the coating while the detachment of *Ulva linza* zoospores remained virtually unaffected (in agreement with previous literature reports[31]). We suggest that under dynamic conditions, dissipation of the diatom's momentum upon impact with the coatings is higher on coatings with low elastic modulus, facilitating attachment. While in essence being a fundamental study, our findings might inspire development of future FRC coatings, as they imply that under dynamic conditions common coatings can be fine-tuned to not only release organisms but also prevent the initial adhesion of soft fouling species.

Conflicts of interest

There are no conflicts to declare.

Data availability

The data supporting this article have been included as part of the SI. See DOI: **https://doi.org/10.1039/d5ma01133g**.

Acknowledgements

References

1 J. A. Callow and M. E. Callow, Trends in the development of environmentally friendly fouling-resistant marine coatings, *Nat. Commun.*, 2011, **2**, 244.

2 J. Bannister, M. Sievers, F. Bush and N. Bloecher, Biofouling in marine aquaculture: a review of recent research and developments, *Biofouling*, 2019, **35**, 631–648.

3 X. Chen, H. Lin, F. Shi, K. Resnik and S. Yi, Membrane Technologies and Applications for Produced Water Treatment, *Solid–Liquid Separation Technologies*, 2022, pp. 123–149, DOI: 10.1201/9781003091011-6.

4 Y. Ibrahim and N. Hilal, A Critical Assessment of Surface-Patterned Membranes and Their Role in Advancing Membrane Technologies, *ACS ES&T Water*, 2023, **3**, 3807–3834.

5 C. Werner, M. F. Maitz and C. Sperling, Current strategies towards hemocompatible coatings, *J. Mater. Chem.*, 2007, **17**, 3376–3384.

6 M. G. Hadfield, Biofilms and Marine Invertebrate Larvae: What Bacteria Produce That Larvae Use to Choose Settlement Sites, *Annu. Rev. Mar. Sci.*, 2011, **3**, 453–470.

7 P.-Y. Qian, A. Cheng, R. Wang and R. Zhang, Marine biofilms: diversity, interactions and biofouling, *Nat. Rev. Microbiol.*, 2022, **20**, 671–684.

8 R. L. Townsin, The Ship Hull Fouling Penalty, *Biofouling*, 2003, **19**, 9–15.

9 M. P. Schultz, J. A. Bendick, E. R. Holm and W. M. Hertel, Economic impact of biofouling on a naval surface ship, *Biofouling*, 2011, **27**, 87–98.

10 M. P. Schultz, Effects of coating roughness and biofouling on ship resistance and powering, *Biofouling*, 2007, **23**, 331–341.

11 M. P. Schultz, Effects of coating roughness and biofouling on ship resistance and powering, *Biofouling*, 2007, **23**, 331–341.

12 IMO. Fourth IMO GHG Study 2020 Full Report. International Maritime Organisation 2021, vol. 6, pp. 951–952.

13 M. Lagerström, E. Ytreberg, A. K. E. Wiklund and L. Granhag, Antifouling paints leach copper in excess – study of metal release rates and efficacy along a salinity gradient, *Water Res.*, 2020, **186**, 116383.

14 C. A. Paz-Villarraga, Í. B. Castro and G. Fillmann, Biocides in antifouling paint formulations currently registered for use, *Environ. Sci. Pollut. Res.*, 2022, **29**, 30090–30101.

15 P. Hu, Q. Xie, C. Ma and G. Zhang, Silicone-Based Fouling-Release Coatings for Marine Antifouling, *Langmuir*, 2020, **36**, 2170–2183.

16 D. M. Yebra, S. Kiil and K. Dam-Johansen, Antifouling technology – Past, present and future steps towards efficient and environmentally friendly antifouling coatings, *Prog. Org. Coat.*, 2004, **50**, 75–104.

17 P. Hu, Q. Xie, C. Ma and G. Zhang, Silicone-Based Fouling-Release Coatings for Marine Antifouling, *Langmuir*, 2020, **36**, 2170–2183.

18 R. F. Brady, Properties which influence marine fouling resistance in polymers containing silicon and fluorine, *Prog. Org. Coat.*, 1999, **35**, 31–35.

19 C. Gay, Some fundamentals of adhesion in synthetic adhesives, *Biofouling*, 2003, **19**, 53–57.

20 J. G. Kohl and I. L. Singer, Pull-off behavior of epoxy bonded to silicone duplex coatings, *Prog. Org. Coat.*, 1999, **36**, 15–20.

21 K. Kendall, The adhesion and surface energy of elastic solids, *J. Phys. D: Appl. Phys.*, 1971, **4**, 320.

22 R. F. Brady and I. L. Singer, Mechanical factors favoring release from fouling release coatings, *Biofouling*, 2000, **15**, 73–81.

23 M. E. Callow and R. L. Fletcher, The influence of low surface energy materials on bioadhesion—a review, *Int. Biodeterior. Biodegrad.*, 1994, **34**, 333–348.

24 R. F. Brady, A fracture mechanical analysis of fouling release from nontoxic antifouling coatings, *Prog. Org. Coat.*, 2001, **43**, 188–192.

25 F. Gubbels, An overview of the chemistry of condensation curing silicone sealants and adhesives, *Int. J. Adhes. Adhes.*, 2024, **132**, 103728.

26 F. Pan, *et al.*, Uncoupling bacterial attachment on and detachment from polydimethylsiloxane surfaces through empirical and simulation studies, *J. Colloid Interface Sci.*, 2022, **622**, 419–430.

27 V. Drebezghova, *et al.*, Initial bacterial retention on polydimethylsiloxane of various stiffnesses: The relevance of modulus (mis)match, *Colloids Surf., B*, 2022, **217**, 112709.

28 H. Straub, F. Zuber, L. Eberl, K. Maniura-Weber and Q. Ren, In Situ Investigation of *Pseudomonas aeruginosa* Biofilm Development: Interplay between Flow, Growth Medium, and Mechanical Properties of Substrate, *ACS Appl. Mater. Interfaces*, 2023, **15**, 2781–2791.

29 J. D. P. Valentin, *et al.*, Substrate viscosity plays an important role in bacterial adhesion under fluid flow, *J. Colloid Interface Sci.*, 2019, **552**, 247–257.

30 J. Sun, *et al.*, Disregarded Free Chains Affect Bacterial Adhesion on Cross-Linked Polydimethylsiloxane Surfaces, *ACS Appl. Mater. Interfaces*, 2023, **15**, 36936–36944.

31 M. K. Chaudhury, J. A. Finlay, J. Y. Chung, M. E. Callow and J. A. Callow, The influence of elastic modulus and thickness on the release of the soft-fouling green alga *Ulva linza* (syn. *Enteromorpha linza*) from poly(dimethylsiloxane) (PDMS) model networks, *Biofouling*, 2005, **21**, 41–48.

32 C. Pretti, *et al.*, An ecotoxicological study on tin- and bismuth-catalysed PDMS based coatings containing a surface-active polymer, *Ecotoxicol. Environ. Saf.*, 2013, **98**, 250–256.

33 A. Kaffashi, A. Jannesari and Z. Ranjbar, Silicone fouling-release coatings: effects of the molecular weight of poly(dimethylsiloxane) and tetraethyl orthosilicate on the magnitude of pseudobarnacle adhesion strength, *Biofouling*, 2012, **28**, 729–741.

34 M. A. Bangoura, *et al.*, Impact of Molecular Weight on Anti-Bioadhesion Efficiency of PDMS-Based Coatings, *Coatings*, 2024, **14**, 149.

35 M. M. Santore, Interplay of physico-chemical and mechanical bacteria-surface interactions with transport processes controls early biofilm growth: A review, *Adv. Colloid Interface Sci.*, 2022, **304**, 102665.

36 F. Song, *et al.*, How Bacteria Respond to Material Stiffness during Attachment: A Role of *Escherichia coli* Flagellar Motility, *ACS Appl. Mater. Interfaces*, 2017, **9**, 22176–22184.

37 J. Koc, *et al.*, Low-Fouling Thin Hydrogel Coatings Made of Photo-Cross-Linked Polyzwitterions, *Langmuir*, 2019, **35**, 1552–1562.

38 H. Jancke, Analysis of silicone resins by methods of ^{29}Si NMR spectroscopy, *Fresenius' J. Anal. Chem.*, 1992, **342**, 846–849.

39 J. Schwarze, R. Wanka and A. Rosenhahn, Microfluidic accumulation assay to quantify the attachment of the marine bacterium *Cobetia marina* on fouling-release coatings, *Biointerphases*, 2020, **15**, 031014.

40 S. Muhring-Salamone, R. Wanka and A. Rosenhahn, Low Fouling Marine Coatings Based on Nitric Oxide-Releasing Polysaccharide-Based Hybrid Materials, *ACS Sustainable Chem. Eng.*, 2023, **11**, 8858–8869.

41 K. A. Nolte, J. Schwarze and A. Rosenhahn, Microfluidic accumulation assay probes attachment of biofilm forming diatom cells, *Biofouling*, 2017, **33**, 531–543.

42 M. P. Schultz, J. A. Finlay, M. E. Callow and J. A. Callow, A turbulent channel flow apparatus for the determination of the adhesion strength of microfouling organisms, *Biofouling*, 2000, **15**, 243–251.

43 M. E. Callow, J. A. Callow, J. D. Pickett-Heaps and R. Wetherbee, Primary adhesion of *Enteromorpha* (Chlorophyta, Ulvales) propagules: quantitative settlement studies and video microscopy, *J. Phycol.*, 1997, **33**, 938–947.

44 K. Sato, The hardness of coating films, *Prog. Org. Coat.*, 1980, **8**, 1–18.

45 M. Heydt, P. Divós, M. Grunze and A. Rosenhahn, Analysis of holographic microscopy data to quantitatively investigate three-dimensional settlement dynamics of algal zoospores in the vicinity of surfaces, *Eur. Phys. J. E: Soft Matter Biol. Phys.*, 2009, **30**, 141–148.

46 M. Heydt, M. E. Pettitt, M. Grunze and A. Rosenhahn, Settlement Behavior of Zoospores of *Ulva linza* During Surface Selection Studied by Digital Holographic Microscopy, *Biointerphases*, 2012, **7**, 33.

47 R. F. Brady and I. L. Singer, Mechanical factors favoring release from fouling release coatings, *Biofouling*, 2000, **15**, 73–81.

48 J. Stein, *et al.*, Structure–Property Relationships of Silicone Biofouling-Release Coatings: Effect of Silicone Network Architecture on Pseudobarnacle Attachment Strengths, *Biofouling*, 2003, **19**, 87–94.